Efficient [^{18}F]AlF radiolabeling of $Z_{HER3:8698}$ affibody molecule for imaging of HER3 positive tumors

Authors:
Chiara Da Pieve‡, Louis Allott‡, Carlos D. Martins, Andrew Vardon, Daniela M. Ciobota, Gabriela Kramer-Marek* and Graham Smith*
Division of Radiotherapy and Imaging, The Institute of Cancer Research, 123 Old Brompton Road, London, SW7 3RP, UK
‡ Author Contributions: Equal contribution for first authorship.
*Corresponding authors: Email: Gabriela.Kramer-Marek@icr.ac.uk, Tel: +44 (0) 2087224412; Graham.Smith@icr.ac.uk, Tel: +44 (0) 2087224482; Fax: +44 (0) 2073705261. The Institute of Cancer Research, 123 Old Brompton Road, London, SW7 3RP, UK

ABSTRACT

The human epidermal growth factor receptor 3 (HER3) is over-expressed in several cancers, being linked to a more resistant phenotype and hence poor patient prognosis. Imaging HER3 is challenging owing to the modest receptor number (<50000 receptors/cell) in overexpressing cancer cells. Therefore, to image HER3 *in vivo*, high target affinity PET probes need to be developed. This work describes two different [^{18}F]AlF radiolabeling strategies of the $Z_{HER3:8698}$ affibody molecule specifically targeting HER3. The one-pot radiolabeling of $Z_{HER3:8698}$ performed at 100ºC and using 1,4,7-triazanonane-1,4,7-triacetate (NOTA) as chelator resulted in radiolabeled products with variable purity attributed to the radioconjugate thermolysis. An alternative approach based on the inverse electron demand Diels-Alder (IEDDA) reaction between a novel tetrazine functionalized 1,4,7-triazacyclononane-1,4-diacetate (NODA) chelator and the *trans*-cyclooctene (TCO) functionalized affibody molecule was also investigated. This method enabled the radiolabeling of the protein at room temperature. The [^{18}F]AlF-NOTA-$Z_{HER3:8698}$ and [^{18}F]AlF-NODA-$Z_{HER3:8698}$ conjugates showed a specific uptake at 1 h after injection in high HER3-expressing MCF-7 tumors of 4.36 ± 0.92 % ID/g and 4.96 ± 0.65 % ID/g respectively. The current results are encouraging for further investigation of [^{18}F]AlF-NOTA-$Z_{HER3:8698}$ as a HER3 imaging agent.

INTRODUCTION

HER3 is a member of the human epidermal growth factor receptor (EGFR/HER) tyrosine kinase family. Its overexpression has been found in a wide variety of cancers including breast, ovary, lung, and head and neck cancer.[1] Multiple studies have highlighted HER3 as a fundamental receptor involved in the establishment of malignancy, demonstrating that HER3 overexpression correlates with advanced disease stage and decreased overall survival.[2-7] Moreover, signaling by HER3 has recently been identified as a prominent mediator of tumor resistance to HER1 and HER2-targeted therapies.[1, 8-11] This has driven the development of HER3-targeting monoclonal antibodies (mAbs), some of which have already entered clinical trials.[12-15] However, the lack of suitable biomarkers to evaluate HER3 status impedes the

effective patient selection for these therapies. Radionuclide-based molecular imaging of HER3 receptor expression could guide patient stratification for HER3 targeted therapies, and more importantly aid monitoring early tumor response to therapeutic intervention. Recently, anti-HER3 mAbs and $F(ab')_2$ fragments were radiolabeled with ^{64}Cu and ^{89}Zr for molecular imaging of HER3 expression.[16-18] Additionally, a ^{89}Zr radiolabeled mAb (GSK2849330) is currently under evaluation in patients with advanced solid tumors (clinical trial identifier: NCT12345174). However, clinical application of full-length radiolabeled antibodies as imaging agents is not optimal because of their long biological half-life and relatively poor tumor penetration which can affect image quality. By contrast, affibody molecules undergo rapid clearance as a result of their smaller size (*ca* 7 kDa), with elimination mainly through the kidneys, increasing the tumor-to-background ratio. Affibody molecules are non-toxic scaffold small proteins characterized by a high binding affinity (K_d in the low-nanomolar to picomolar range) and high target specificity. Furthermore, the introduction of a unique cysteine residue at the C-terminus of the molecules allows the site-specific conjugation of chelators, dyes or radiolabeled groups to the protein.[19, 20] The high affinity affibody molecule $Z_{HER3:8698}$ has been previously selected and radiolabeled with the single photon emission computed tomography (SPECT) radioisotopes ^{99m}Tc and ^{111}In in order to image HER3 expression *in vivo*.[21-23] To successfully visualize the receptor, the authors had to overcome a variety of challenges including the modest overexpression of the HER3 target (*ca* 50000 receptors/cell in high-expressing cell lines such as BT-474) and the natural high expression of HER3 in normal organs and tissues (such as intestine, salivary glands and lung).[22, 24] Additionally, the same research group reported that the affibody molecule uptake in tumors having modest receptor overexpression is highly influenced by the injected protein dose. They identified 1 µg of radiolabeled protein to be the optimal quantity for HER3 imaging, since higher amounts, associated to lower specific activity, resulted in diminished tumor uptake.[25]his study describes the development of affibody-based agents suitable for ^{18}F positron emission tomography (PET) imaging of HER3-expression. Because of its half-life (109 minutes), the PET radionuclide fluorine-18 is more compatible with the pharmacokinetics of the affibody molecule than SPECT radioisotopes enabling the acquisition of high quality PET images at 1-3 hours post injection. The affibody molecule $Z_{HER3:8698}$ was radiolabeled using the rapid and efficient aluminum ^{18}F-fluoride ($[^{18}F]AlF$) approach, based on the formation of a stable ^{18}F-aluminum bond, and consequent coordination by macrocyclic ligands.[26, 27] The $[^{18}F]AlF$ radiolabeling method can be performed in a single step (one-pot reaction) and it has been used to successfully radiolabel a variety of peptides and proteins including affibody molecules.[28-35] Two different radiolabeling strategies were investigated to establish the best protocol for a reproducible production of $[^{18}F]AlF$ radiolabeled $Z_{HER3:8698}$ suitable for imaging HER3 expression. Firstly, the synthesis reported in the literature using NOTA as the chelator for the $[^{18}F]AlF$ complex was followed.[36] Secondly, the inverse electron demand Diels-Alder (IEDDA) reaction to radiolabel the affibody molecule under mild reaction conditions in a two-step method was adopted. McBride *et al.* reported the radiolabeling of a heat-sensitive antibody Fab' fragment using the maleimide functionalized 1,4,7-triazacyclononane-1,4-diacetate chelator (NODA-MPAEM) which was mixed with Al^{3+} and $[^{18}F]F^-$ and then conjugated to the reduced thiol group of the protein.[37] Kiesewetter *et al.* employed a similar maleimide-thiol conjugation

approach to synthesize the affibody-based radioconjugate [^{18}F]FBEM-$Z_{HER2:342}$. A limitation of this approach is that an initial reduction of the thiol group of the terminal cysteine of the affibody molecule was required as part of the radiolabeling protocol. The reducing agent had to be removed by size exclusion chromatography prior to conjugation of the reduced affibody molecule with the maleimide functionalized prosthetic group; as a result, the radiolabeling reaction lasted more than an hour and required multiple purification steps.[38] The IEDDA reaction is an attractive alternative to the maleimide-thiol conjugation because it eliminates the need for the reduction step as part of the radiolabeling procedure. This approach, which is based on the reaction between a tetrazine and a strained cycloalkene, is chemospecific, proceeds in aqueous medium at room temperature, and forms stable products with negligible side products.[39] These characteristics have prompted an increased interest in IEDDA reactions for bioconjugation as well as pretargeting purposes.[39-41] To perform this synthetic methodology, the novel [^{18}F]AlF-**3**, containing the NODA chelator instead of NOTA, was prepared and subsequently reacted with the TCO-functionalized-affibody molecule at room temperature *via* an IEDDA reaction. This methodology enables the radiofluorination of heat-sensitive compounds.

The two different strategies described above were developed for the [^{18}F]AlF radiolabeling of the HER3 targeting affibody molecule $Z_{HER3:8698}$ with a particular focus on protein stability and radiolabeling efficiency (expressed as specific activity of the final radiocojugates). The performance *in vitro* and *in vivo* of both radioligands has been further compared using high HER3-expressing MCF-7 human breast cancer cells and tumor xenografts.

RESULTS AND DISCUSSION

Synthesis of the affibody conjugates. When analyzed by RP-HPLC, the affibody molecule having a cysteine residue at its C-terminus ($Z_{HER3:8698}$-Cys) was observed to be present in solution mostly in a dimeric form due to the formation of an intermolecular disulfide bond (Figure S1A). In order to proceed with the conjugation using the maleimide functionalized NOTA or TCO, the affibody dimer required reduction to its monomeric free sulfhydryl form (Figure S1B). Different protocols described in the literature use an excess of a reducing agent such as DTT or TCEP-HCl which is then removed by gel permeation chromatography using either NAP-5 or Zeba columns just before proceeding to the conjugation reaction.[38, 42] When such procedures were followed for the present study, the outcome was a substantial loss of affibody molecule because of the similarity between its molecular weight and the MWCO of the columns. The protein loss was found to be more prominent when low sample volumes and low protein concentrations were used. Moreover, the protein was usually recovered from size exclusion columns in a more diluted solution requiring the addition of a molar excess of maleimide functionalized compounds (i.e. MMA-NOTA and TCO-PEG_3-Maleimide) which had to be subsequently removed by gel permeation chromatography. Added to the loss of protein, this overall multi-step process was found to be time consuming and required the use of multiple size exclusion columns. To improve the product yield and simplify its purification, a one-pot conjugation reaction was developed using TCEP-HCl as the reducing agent, which was not removed from the mixture. A quantitative yield of the products NOTA-$Z_{HER3:8698}$ and TCO-$Z_{HER3:8698}$ in the shortest time possible was thus achieved, indicated by

the disappearance of the starting material when analyzed by RP-HPLC (Figures S1, S2A and S3A). To attain extremely pure products for the radiolabeling reaction, a single final purification of the conjugates by semi-preparative RP-HPLC was performed (Figures S2B and S3B). Following this optimized synthetic method, the pure products were obtained in a *ca* 60% and *ca* 45% yield for NOTA-$Z_{HER3:8698}$ and TCO-$Z_{HER3:8698}$ conjugates respectively compared to the 15-30% yield obtained when conventional methods were utilized. All products were characterized by MALDI-mass spectrometry (Supporting Information).

Synthesis of NODA-tetrazine (3). The design of the tetrazine-chelator construct was dictated by the hydrophilicity of the final affibody conjugate and the synthetic accessibility of the chosen tetrazine. Therefore, a small molecular weight tetrazine-chelator having the closest structure to MMA-NOTA was developed. The non-commercially available tetrazine **1** was synthesized in a simple one step process following a literature procedure.[43] The NODA macrocycle was selected because it showed a higher labeling efficiency compared to NOTA, believed to be caused by the absence of a destabilizing electron-withdrawing carbonyl adjacent to a coordinating nitrogen atom of the macrocycle.[41] The tosylated tetrazine **2** was reacted with NO2AtBu and subsequently deprotected using TFA yielding the NODA-containing tetrazine **3** (Scheme 1). The final product was purified by RP-HPLC to ensure a high purity material for the subsequent radiolabeling (Figure S4).

Scheme 1. Preparation of tetrazines **2** and **3** and radiolabelling of tetrazine **3**.

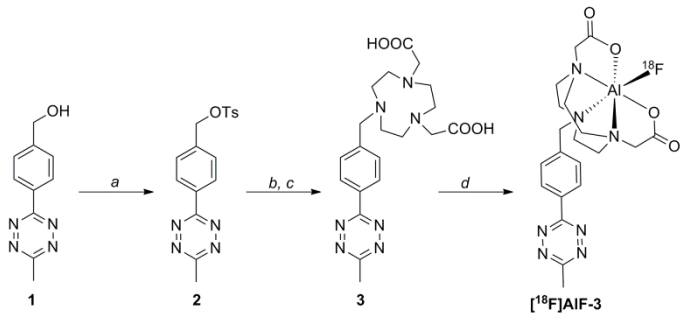

Reaction conditions: (*a*) *p*-toluenesulfonyl chloride, 16 h, rt; (*b*) NO2AtBu, DIPEA, 24 h, rt; (*c*) TFA, 3h, rt. (*d*) $AlCl_3$, $[^{18}F]F^-$, sodium acetate/ethanol 1:1 (v/v), pH4, 15 min, 100ºC

[^{18}F]AlF radiolabeling of NOTA-$Z_{HER3:8698}$ and NODA-$Z_{HER3:8698}$. The two different radiochemical methodologies investigated for the radiolabeling of $Z_{HER3:8698}$ with the [^{18}F]AlF complex are shown in Scheme 2. Initially, a conventional direct radiolabeling strategy of the NOTA-$Z_{HER3:8698}$ affibody conjugate was carried out with [^{18}F]AlF in a one-pot reaction at pH 4, 100ºC for 15 min using ethanol as organic co-solvent (50% v/v) as the addition of a hydrophilic organic solvent showed to increase the radiolabeled product yield.[32, 33, 36] The radiochemical conversion and the specific activity of the radioconjugate were 38.8 ± 5.8 % (non-decay corrected) and 0.8-1.5 MBq/µg (6.0-11.9 GBq/µmol) respectively (Figure S13).

Scheme 2. Preparation of radioconjugates [^{18}F]AlF-NOTA-$Z_{HER3:8698}$ (**A**) and [^{18}F]AlF-NODA-$Z_{HER3:8698}$ (**B**).

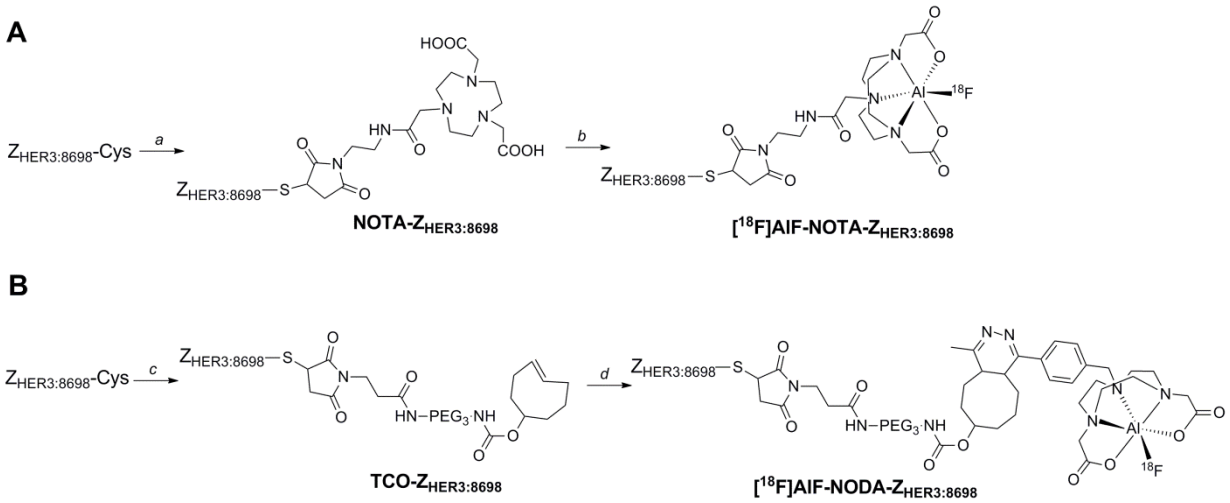

Reaction conditions: (*a*) TCEP-HCl, MMA-NOTA, PBS; (*b*) $AlCl_3$, [^{18}F]F^-, sodium acetate/ethanol 1:1 (v/v), pH4, 15 min, 100ºC; (*c*) TCEP-HCl, TCO-PEG_3-Maleimide, PBS; (*d*) 17 min, rt.

Mirroring Glaser *et al.*, it was observed that optimal radiolabeling efficiencies were achieved by heating the [^{18}F]AlF-complexation reaction at 100°C in conjunction with the formation of a by-product assumed to originate from the decomposition of the radioconjugate (Figure 1A).[33] Therefore, a procedure comprising of RP-HPLC followed by HLB-SPE purification was developed to produce [^{18}F]AlF-NOTA-$Z_{HER3:8698}$ with a RCP > 98% verified by HPLC (Figure 1B and Figure S5). To confirm its purity, the isolated product was analyzed using radio-SDS-PAGE and silver staining. Only one band corresponding to the molecular weight of the monomeric affibody molecule was detected on the gel autoradiography. No other bands which could indicate aggregation of the radioconjugate (high molecular weight compounds) or degradation (low molecular weight species) were observed (Figure S15).

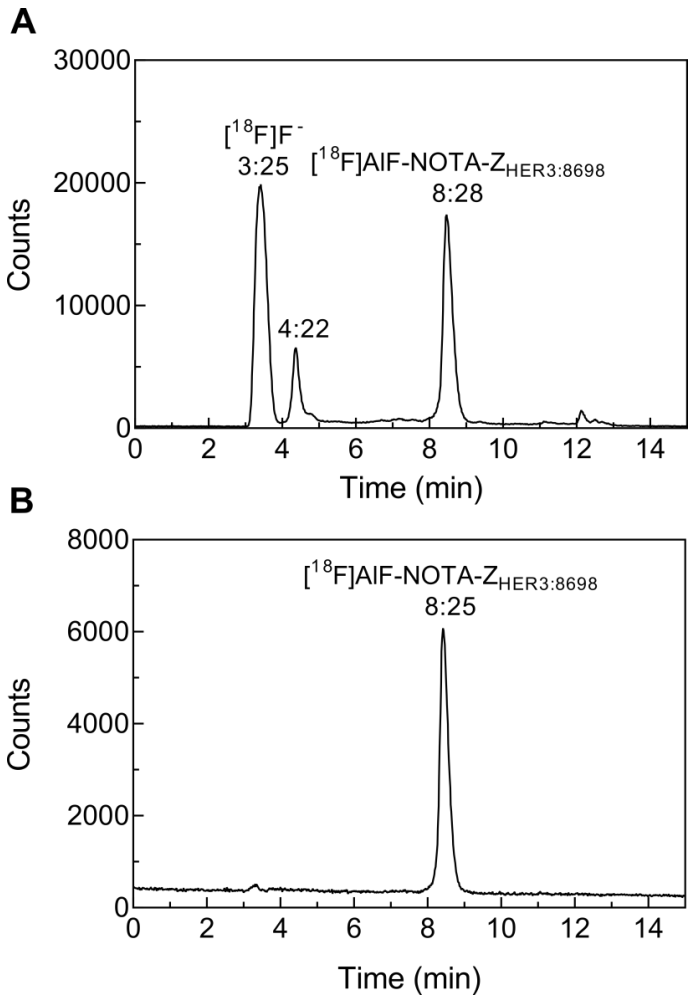

Figure 1. Radiochromatograms of [^{18}F]AlF-NOTA-$Z_{HER3:8698}$ reaction mixture (**A**) and isolated product (**B**). Free ^{18}F-fluoride and the radioconjugate elute with a R_t of 3:25 and 8:28 respectively. The peak with R_t 4:22 is the side-product from the thermolysis. The retention times (R_t) are expressed as min:sec.

The alternative two-step approach first required the radiolabeling of the tetrazine-bearing NODA chelator (**3)** with the [^{18}F]AlF complex followed by the IEDDA reaction with the TCO-functionalized $Z_{HER3:8698}$ affibody molecule (Scheme 2). Crucially, the mild conjugation conditions used in the IEDDA reaction can limit the formation of the by-product (Figure 1A, product eluting at 4:22) caused by the exposure of the conjugate to the high temperatures required for radiolabeling step. [^{18}F]AlF-**3** was prepared in high RCC (70-95%, calculated by HPLC and non-decay corrected) in a one pot reaction using ethanol as organic co-solvent (50% v/v). To confirm the hydrophilicity of [^{18}F]AlF-**3**, its distribution coefficient (logD) between PBS (pH 7.4) and *n*-octanol was determined (Supporting Information). The $logD_{7.4}$ was found to be -1.87 ± 0.01 which confirmed that the product possessed suitable hydrophilicity for further investigation. The radio-HPLC of [^{18}F]AlF-**3** shows the presence of predominantly the two species [^{18}F]AlF-**3A** and [^{18}F]AlF-**3B** (Figure 2). When analyzed immediately after the end of reaction, the mixture was composed of mainly the product

eluting at 7 min 55 seconds ([^{18}F]AlF-**3B**) with a minimal amount of product having a retention time of 7 min 11 seconds ([^{18}F]AlF-**3A**). The [^{18}F]AlF-**3B**/**A** ratio (based on peak areas) was found to be generally in the range of 11-23. After 2 hours, the ratio decreased to as little as 0.26 indicating that [^{18}F]AlF-**3B** converted into [^{18}F]AlF-**3A** over time, although not completely. The same behavior was observed when the radiolabeling was carried out in buffer without ethanol (Figure S6). Alternative organic co-solvents to ethanol (i.e. acetonitrile, *tert*-butanol) produced the same number of [^{18}F]AlF-**3** forms which surprisingly did not convert over time (Figure S7 and S8). A similar NODA-derivative, lacking the tetrazine moiety, showed a single radioactive product when radiolabeled and analyzed by RP-HPLC (data not shown) indicating the involvement of the tetrazine in the generation of the two species. This was further confirmed by the formation of a comparable set of products when a similar compound, but having a longer linker between the NODA chelator and the tetrazine moiety, was radiolabeled and analyzed by RP-HPLC (data not shown).

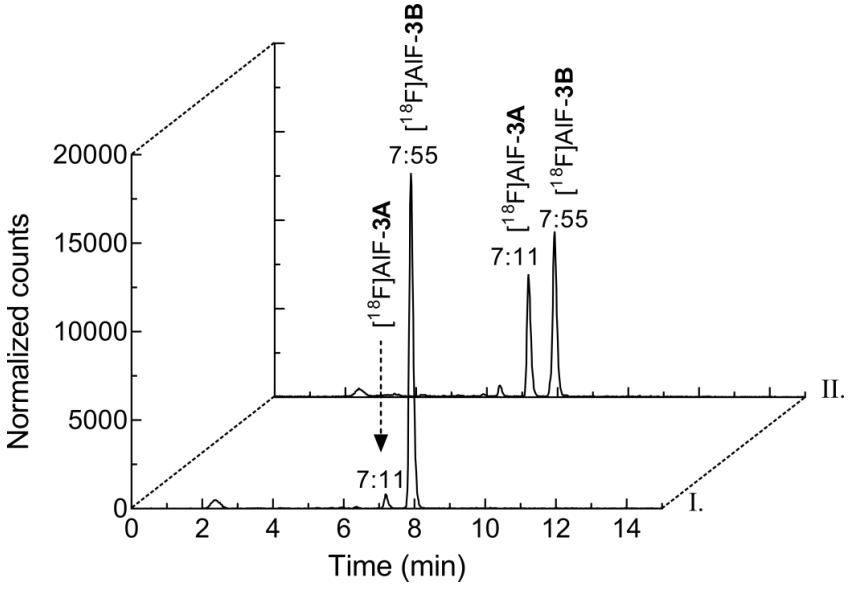

Figure 2. Radiochromatograms of [^{18}F]AlF-**3** as a mixture of [^{18}F]AlF-**3A** and [^{18}F]AlF-**3B**. The alteration in composition is depicted as a function of time. In the displayed representative radiotraces, the [^{18}F]AlF-**3B**/**A** ratio is 23.4 immediately after the end of the reaction (I.) and it decreases to 1.36 after 2 h, rt (II.). The retention times (R_t) are expressed as min:sec.

The precise molecular structures for [^{18}F]AlF-**3A** and [^{18}F]AlF-**3B** are uncertain at present and will be the subject of further study.

Non-purified [^{18}F]AlF-**3** was reacted with lyophilized TCO-$Z_{HER3:8698}$ in a 7:1 molar ratio at room temperature yielding the product almost quantitatively (Figure S9). RP-HPLC followed by HLB-SPE were used to purify the final product [^{18}F]AlF-NODA-$Z_{HER3:8698}$ from the excess of [^{18}F]AlF-**3** and free ^{18}F-fluoride. As shown in Figure 3 and Figure S10, the IEDDA reaction yielded two radiolabeled products identified by HPLC.

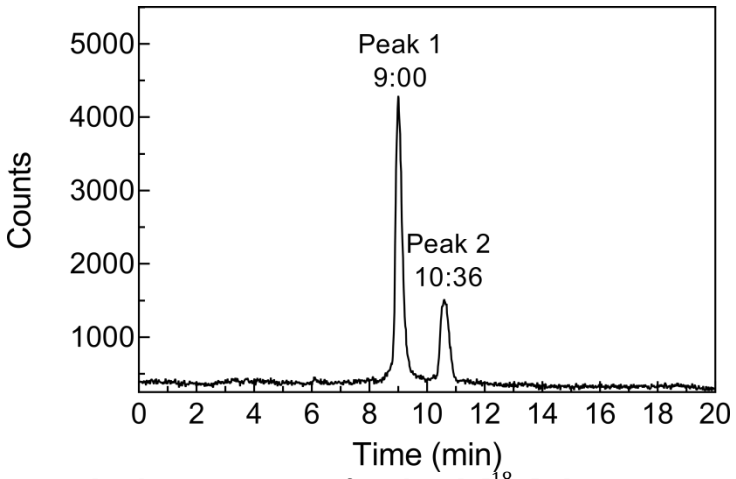

Figure 3. Radiochromatogram of isolated [^{18}F]AlF-NODA-$Z_{HER3:8698}$. The retention times (R_t) are expressed as min:sec.

At this stage, an investigation on whether the formation of the IEDDA adducts was dependent on the species composition of [^{18}F]AlF-**3** was carried out. [^{18}F]AlF-**3A** and [^{18}F]AlF-**3B** were hence collected separately by HPLC and, after confirming that no conversion was occurring once isolated (Figure S11), they were incubated with an excess of TCO-$Z_{HER3:8698}$. HPLC analysis of the reaction mixtures showed that [^{18}F]AlF-**3A** did not react with TCO-$Z_{HER3:8698}$ even after 4 hours (Figure S12A). Conversely, [^{18}F]AlF-**3B** reacted with the TCO-affibody conjugate generating the previously described multiple peaks pattern (Figure 3 and Figure S12B). The reason behind the inactivity of product [^{18}F]AlF-**3A** is under investigation. To reduce its effect on the yield of the final radioconjugate, it was necessary to either add the freshly prepared [^{18}F]AlF-**3** to TCO-$Z_{HER3:8698}$ promptly or synthesize [^{18}F]AlF-**3** using an alternative organic co-solvent to ethanol to prevent species interconversion.
The two peaks from the IEDDA adduct [^{18}F]AlF-NODA-$Z_{HER3:8698}$ were collected separately by HPLC and investigated further. When the peak having a R_t of 9 min (Peak 1, Figure 3) was reinjected, one single product with matching retention time to the one in the original separation was detected (Figure S13A). Attempts to isolate the peak at 10 min 36 sec (Peak 2, Figure 3) were unsuccessful. Each trial resulted in a mixture of the two peaks suggesting that Peak 2 partially transforms into Peak 1 over time (Figure S13B). Selvaraj *et al* suggested that by reacting with water, the IEDDA ligation product [^{18}F]AlF-NODA-$Z_{HER3:8698}$-Dihydropyridazine undergoes a series of structural rearrangements that ultimately leads to the stable aromatic [^{18}F]AlF-NODA-$Z_{HER3:8698}$-Pyridazine (Scheme 3).[44] Therefore, when analyzed by HPLC the radioconjugate is present as a combination of the aromatized [^{18}F]AlF-NODA-$Z_{HER3:8698}$-Pyridazine (Peak 1, Figure 3) and of [^{18}F]AlF-NODA-$Z_{HER3:8698}$-Dihydropyridazine (Peak 2, Figure 3). Furthermore, when [^{18}F]AlF-NODA-$Z_{HER3:8698}$ was analyzed as a mixture by radio-SDS-PAGE only a single band with a comparable molecular weight to the $Z_{HER3:8698}$ affibody was visible. This indicated that neither of the two products (Peak1 and Peak2) was the result of either aggregation or degradation of the protein (Figure S17). [^{18}F]AlF-NODA-$Z_{HER3:8698}$ was isolated in high radiochemical purity exceeding 98% (Figure 3) and the specific activity was in general higher than the NOTA radioconjugate but over a large range (0.7-2.3 MBq/µg; 5.5-18.4 GBq/µmol) (Figure S14) which may be due to the inconsistent quantity of inert product present in [^{18}F]AlF-**3**. To investigate the impact of

the IEDDA ligation adduct on [^{18}F]AlF-NODA-$Z_{HER3:8698}$ hydrophilicity, its log$D_{7.4}$ value was determined and compared to [^{18}F]AlF-NOTA-$Z_{HER3:8698}$ (Supporting Information). The log$D_{7.4}$ for [^{18}F]AlF-NODA-$Z_{HER3:8698}$ was found to be hydrophilic with a value of -1.87 ± 0.07; however, with a log$D_{7.4}$ value of -2.19 ± 0.01, [^{18}F]AlF-NOTA-$Z_{HER3:8698}$ proved to be the most hydrophilic of the radioconjugates.

Scheme 3. IEDDA ligation products of the reaction between [^{18}F]AlF-**3** and TCO-$Z_{HER3:8698}$.

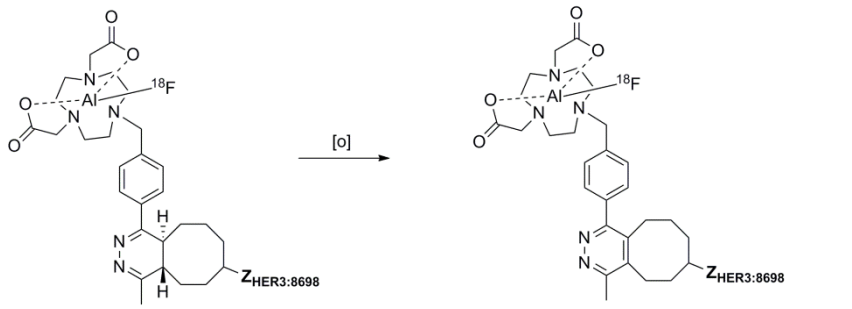

[^{18}F]AlF-NODA-$Z_{HER3:8698}$-Dihydropyridazine [^{18}F]AlF-NODA-$Z_{HER3:8698}$-Pyridazine

***In vitro* stability studies.** The stability of [^{18}F]AlF-NOTA-$Z_{HER3:8698}$ and [^{18}F]AlF-NODA-$Z_{HER3:8698}$ was determined by incubating the radioconjugates in mouse serum at 37°C. By HPLC analysis, it was found that 97.9 ± 0.5% of [^{18}F]AlF-NOTA-$Z_{HER3:8698}$ and 91.5 ± 1.2% of [^{18}F]AlF-NODA-$Z_{HER3:8698}$ remained intact after 1 h (Figures S15). In both cases, the release of ^{18}F (most probably in the form of the [^{18}F]AlF complex) was observed as the main product of decomposition of the radioligands with [^{18}F]AlF-NODA-$Z_{HER3:8698}$ less stable to degradation. However, due to the short blood half-life of the affibody molecule, it is improbable that the breakdown of the radioconjugate would have a significant impact on its further *in vivo* validation.[45] Notably, the HPLC trace of [^{18}F]AlF-NODA-$Z_{HER3:8698}$ (Figure S15B) shows the presence of two peaks (Peak 1 and Peak 2, Figure 3) corresponding to [^{18}F]AlF-NODA-$Z_{HER3:8698}$-Dihydropyridazine and [^{18}F]AlF-NODA-$Z_{HER3:8698}$-Pyridazine as previously described (Scheme 3). This confirms that the radioconjugate is present as a mixture in physiological conditions. A residual activity associated with the pelleted protein (20 ± 0.1% and 18.3 ± 2.3% for [^{18}F]AlF-NOTA-$Z_{HER3:8698}$ and [^{18}F]AlF-NODA-$Z_{HER3:8698}$ respectively) shows some non-specific affinity of the radiotracers towards the serum protein. Having a less than 50% binding affinity value, both radioconjugates can be considered as low plasma protein binding compounds.[46]

***In vitro* receptor binding.** A saturation binding assay was performed to estimate the dissociation constant (K_d) of the two ^{18}F-radiolabeled conjugates using high HER3-expressing MCF-7 cells. The K_d was found to be 0.44 ± 0.04 nM for [^{18}F]AlF-NOTA-$Z_{HER3:8698}$ and 1.01 ± 0.28 nM for [^{18}F]AlF-NODA-$Z_{HER3:8698}$ (Figure S18). Furthermore, a specificity of binding assay showed that both radiolabeled conjugates recognize the HER3 receptor present on MCF-7 cells (Figure 4). A significant decrease in cell-associated radioactivity achieved by either pre-incubating MCF-7 cells with 100-fold molar excess of the non-radiolabeled affibody molecule or using low HER3-expressing MDA-MB-231 cells confirmed the target specificity (Figure 4).

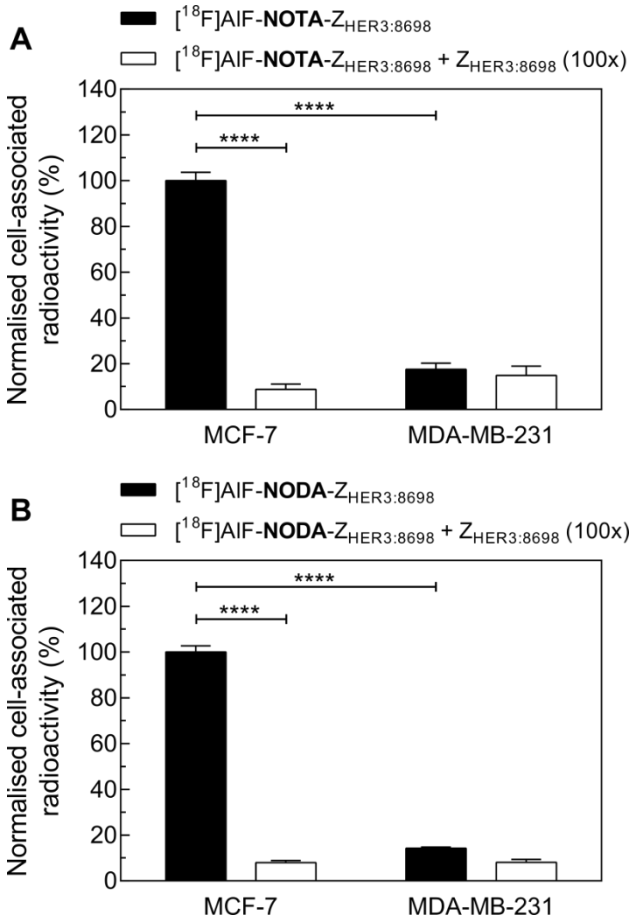

Figure 4. *In vitro* binding specificity of [^{18}F]AlF-NOTA-$Z_{HER3:8698}$ (**A**) and [^{18}F]AlF-NODA-$Z_{HER3:8698}$ (**B**) to MCF-7 and MDA-MB-231 cells. The data are shown as the mean values of n = 3 experiments ± SEM. Statistical significance was determined with a two-way ANOVA with Tukey correction ($^{****}P < 0.0001$).

***In vivo* evaluation.** The targeting properties of [^{18}F]AlF-NOTA-$Z_{HER3:8698}$ and [^{18}F]AlF-NODA-$Z_{HER3:8698}$ were evaluated in high HER3-expressing MCF-7 tumor-bearing mice. The biodistribution of both radioconjugates 1 h after injection displays similar *in vivo* behavior and pharmacokinetic profiles (Table 1). A relatively high accumulation in the tumor (4.36 ± 0.92 and 4.96 ± 0.92 %ID/g for [^{18}F]AlF-NOTA-$Z_{HER3:8698}$ and [^{18}F]AlF-NODA-$Z_{HER3:8698}$ respectively) was found when 1 µg of protein (*ca* 0.8 MBq) was injected. The kidney uptake was high, resulting from the predominant renal excretion of the affibody molecule. This accumulation is the consequence of the reabsorption of the radiolabeled affibody molecule from the renal ultrafiltrate in the proximal tubules, where it is subsequently degraded. The radioactive metabolites are retained by the proximal tubular cells resulting in a renal accumulation of radioactivity over time.[47] Both radioconjugates also showed high uptake in naturally HER3-expressing organs such as lungs, liver and intestine. Notably, [^{18}F]AlF-NODA-$Z_{HER3:8698}$ showed an increased accumulation in the intestine (24.77 ± 13.96 %ID/g compared to 12.42 ± 3.35 %ID/g for [^{18}F]AlF-NOTA-$Z_{HER3:8698}$) suggesting that some hepatobiliary excretion might be involved in its clearance most likely due to the slightly

increased lipophilicity of [^{18}F]AlF-NODA-$Z_{HER3:8698}$. Similarly, blood, spleen, pancreas, bone and muscle uptakes were higher than those of [^{18}F]AlF-NOTA-$Z_{HER3:8698}$ (Table 1). However, in contrast to the other HER3 targeting affibody based radioligands reported in the literature, high-contrast images were achieved using both radioconjugates already 1 h after injection.[22, 23, 48] The biodistribution pattern of [^{18}F]AlF-NOTA-$Z_{HER3:8698}$ produced tumor/blood, tumor/bone and tumor/muscle ratios of 24.61 ± 14.45, 20.86 ± 1.15, and 34.96 ± 8.60 respectively which are higher than the values obtained for [^{18}F]AlF-NODA-$Z_{HER3:8698}$ (Table 2).These findings suggest that [^{18}F]AlF-NOTA-$Z_{HER3:8698}$ may be considered the most promising candidate as HER3 imaging agent. Additionally, when low-HER3 expressing MDA-MB-231 tumor-bearing mice were injected with [^{18}F]AlF-NOTA-$Z_{HER3:8698}$ the tumor uptake was significantly reduced to 0.46 ± 0.02 %ID/g at 1 h p.i. (Table 1 and Figure 5) confirming the *in vivo* binding specificity of the radioconjugate.

Table 1. Biodistribution results for [^{18}F]AlF-NOTA-$Z_{HER3:8698}$ and [^{18}F]AlF-NODA-$Z_{HER3:8698}$ (0.8 MBq/mouse) at 1 h p.i. The data are reported as the mean percentage of the injected probe dose per gram of tissue (%ID/g) ± SD (for each group, n = 3). Statistical significance was determined with an unpaired t-test with Welch's correction.

	[^{18}F]AlF-NODA-$Z_{HER3:8698}$	**[^{18}F]AlF-NOTA-$Z_{HER3:8698}$**	
Tissue	**MCF-7**	**MCF-7**	**MDA-MB-231**
Blood	0.67 ± 0.47	0.25 ± 0.21	0.15 ± 0.04
Heart	0.52 ± 0.30	0.23 ± 0.01	0.25 ± 0.07
Lungs	2.05 ± 0.11	2.26 ± 0.88	2.42 ± 0.04
Kidney	118.67 ± 2.85	134.78 ± 28.53	167.47 ± 1.83
Spleen	0.43 ± 0.32	0.20 ± 0.03	0.23 ± 0.01
Liver	6.92 ± 3.92	5.65 ± 0.92	7.23 ± 0.35
Pancreas	1.97 ± 1.85	0.51 ± 0.24	0.85 ± 0.02
Tumor	4.96 ± 0.65	4.36 ± 0.92	0.46 ± 0.02[a]
Bone	0.38 ± 0.19	0.21 ± 0.06	0.21 ± 0.0001
Small Intestine	24.77 ± 13.96	12.42 ± 3.35	25.16 ± 2.8
Muscle	0.29 ± 0.10	0.13 ± 0.04	0.11 ± 0.01

[a] Significantly lower uptake ($P < 0.001$) in MDM-MB-231 tumors.

Table 2. Tumor-to-organ ratios at 1h p.i. of [^{18}F]AlF-NOTA-$Z_{HER3:8698}$ and [^{18}F]AlF-NODA-$Z_{HER3:8698}$.

	[^{18}F]AlF-NODA-$Z_{HER3:8698}$	[^{18}F]AlF-NOTA-$Z_{HER3:8698}$
Tissue	**MCF-7**	**MCF-7**
Blood	9.27 ± 4.02	24.61 ± 14.45
Heart	11.10 ± 3.96	19.18 ± 5.10
Lungs	2.42 ± 0.25	2.01 ± 0.34
Kidney	0.04 ± 0.01	0.03 ± 0.01
Spleen	14.99 ± 6.78	21.36 ± 1.60
Liver	0.86 ± 0.42	0.77 ± 0.06
Pancreas	3.90 ± 2.27	11.66 ± 9.75
Tumor	-	-
Bone	14.36 ± 4.81	20.86 ± 1.15
Small Intestine	0.25 ± 0.13	0.36 ± 0.04
Muscle	18.01 ± 3.31	34.96 ± 8.60

The representative PET images of MCF-7 tumor-bearing mice at 1 h after injection of [^{18}F]AlF-NOTA-$Z_{HER3:8698}$ and [^{18}F]AlF-NODA-$Z_{HER3:8698}$ are shown in Figure 5. Both radioconjugates, but in particular [^{18}F]AlF-NOTA-$Z_{HER3:8698}$, allowed a clear visualization of the tumor as a result of the high signal-to-noise ratio. In agreement with the biodistribution data, the signal intensity in the kidneys was very high in both cases.

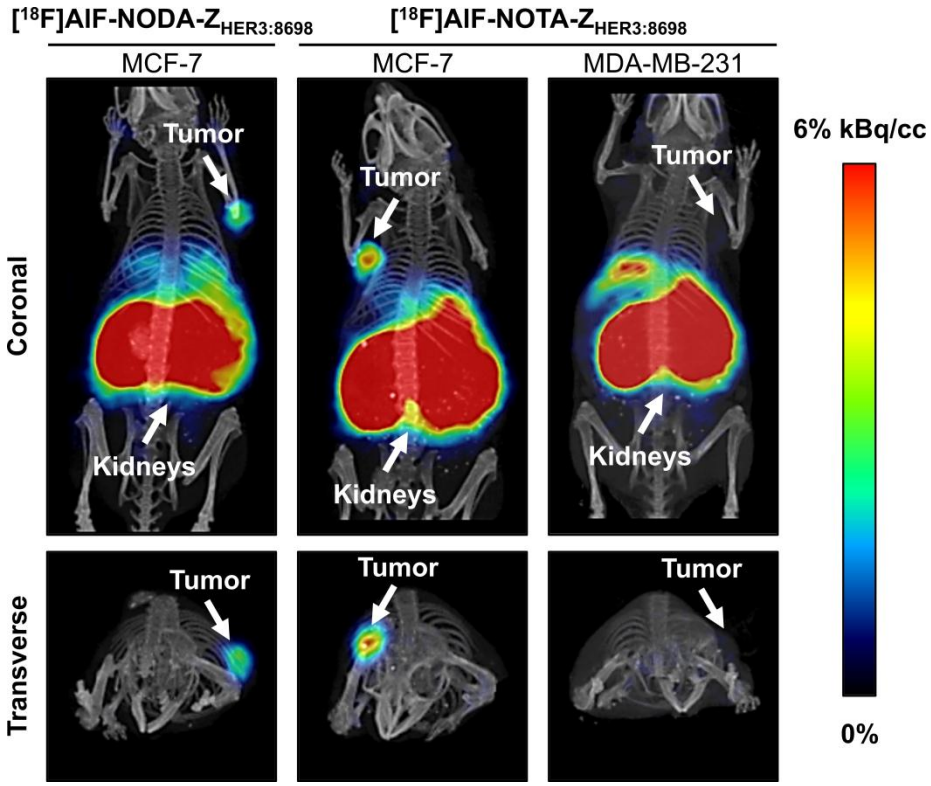

Figure 5. PET/CT images of MCF-7 tumor-bearing mice using [^{18}F]AlF-NODA-$Z_{HER3:8698}$ and [^{18}F]AlF-NOTA-$Z_{HER3:8698}$. High contrast images were acquired as early as 1 h p.i. When [^{18}F]AlF-NOTA-$Z_{HER3:8698}$ was injected in low-HER3 expressing MDA-MB-231 tumor-

bearing mice the tumor uptake was significantly reduced confirming the binding specificity of the radioconjugate.

CONCLUSIONS

Two strategies for the ^{18}F-radiolabeling of the HER3-binding affibody molecule $Z_{HER3:8698}$ have been described: a conventional one-pot reaction at 100ºC using NOTA as chelator for the [^{18}F]AlF complex, and an alternative two-step approach based on the IEDDA reaction using a novel tetrazine functionalized NODA and performed at room temperature. Both methods lead to an efficient incorporation of ^{18}F and produced high purity radiolabeled products (RCP > 98%) after following the same purification procedure. Compared to conventional radiolabeling, the IEDDA approach helped avoid thermal degradation of the radioconjugate and can be used to radiolabel heat-sensitive compounds. However, this method generated multiple species, one of which was unreactive with the targeting affibody molecule. Although the successful tumor targeting and fast blood clearance of both radioconjugates ([^{18}F]AlF-NOTA-$Z_{HER3:8698}$ and [^{18}F]AlF-NODA-$Z_{HER3:8698}$) enabled the clear visualization of high HER3-expressing MCF-7 tumors as early as 1 h p.i., the biodistribution of [^{18}F]AlF-NODA-$Z_{HER3:8698}$ was sub-optimal compared to [^{18}F]AlF-NOTA-$Z_{HER3:8698}$. However, because of their equally high tumor uptake, studies to evaluate the effectiveness of either [^{18}F]AlF-NOTA-$Z_{HER3:8698}$ or [^{18}F]AlF-NOTA-$Z_{HER3:8698}$ to monitor anti-HER3 targeted therapies are on-going.

EXPERIMENTAL PROCEDURES

Conjugation of MMA-NOTA to $Z_{HER3:8698}$-Cys affibody molecule. In a 1.5 mL low protein binding centrifuge tube, a solution of $Z_{HER3:8698}$-Cys (300 µL, 1.6 mg/mL in PBS, 68.4 nmol) was diluted with PBS (130 µL) and EDTA 0.1 M solution (40 µL). A freshly prepared solution of TCEP-HCl (9.8 µL, 0.05 mg/µL in PBS, 1.71 µmol) was added and the mixture was incubated in a Thermomixer at 85°C for 5 min (800 rpm) followed by 25 min at room temperature. MMA-NOTA was then added (1.3 mg, 2.4 µmol) and the solution was incubated in a Thermomixer at 37°C for 2 h (800 rpm). The reaction mixture was analyzed by analytical reverse phase high performance liquid chromatography using gradient A (Supporting Information). The product was purified by semi-preparative RP-HPLC. The collected fractions containing the product were lyophilized and quantified by measuring the UV absorbance at 280 nm on a Nanodrop 2000 (310 µg, 61% yield). Analytical RP-HPLC: R_t = 8:32 (min:sec) MALDI-MS (*m/z*) : $[M + H]^+$ expected: 7434, found: 7434.2

Radiosynthesis of [^{18}F]AlF-NOTA-$Z_{HER3:8698}$. To a 1.5 mL low protein binding plastic tube containing the lyophilized NOTA-$Z_{HER3:8698}$ (10 nmol), 2 mM $AlCl_3$ (3.5-5.0 µl, 7-10 nmol) in 0.5 M NaOAc buffer pH 4, and aqueous non-purified ^{18}F-fluoride (250-300 MBq), followed by an equal volume of ethanol, were added. The mixture was heated at 100°C for 15 min. After cooling to ambient temperature, the solution was diluted with 0.1% aq TFA (50 µl) and purified by RP-HPLC using Gradient A (Supporting Information): R_t = 8.53 (min:sec). The collected fraction containing the product was diluted with 0.1% aq TFA (3

mL) and loaded on an Oasis HLB-SPE cartridge (1 mL, 30 mg). The trapped radioactivity was washed with 0.1% aq TFA (5 mL) and then eluted with of 50% ethanol/water (v/v, 100 µl). The product was quantified by measuring the UV absorbance at 280 nm on a Nanodrop 2000. Synthesis time (from the beginning of the reaction) = *ca* 50 min. The RCC (non-decay corrected) was expressed as the mean of n = 9 experiments ± SD. Protein recovery = 12.5-42.6%; RCY = 9.9-27.4%

Conjugation of TCO-PEG$_3$-Maleimide to Z$_{HER3:8698}$-Cys affibody molecule. In a low protein binding 1.5 mL low protein binding centrifuge tube, a solution of Z$_{HER3:8698}$-Cys (300 µL, 1.6 mg/mL in PBS, 68.4 nmol) was diluted with PBS (130 µL) and 0.1 M EDTA solution (40 µL). A freshly prepared solution of TCEP-HCl (9.8 µL, 0.05mg/µL in PBS, 1.71 µmol) was added and the mixture was incubated in a Thermomixer at 85°C for 5 min (800 rpm) followed by 25 min at 21°C. A solution of TCO-PEG$_3$-Maleimide in DMSO (40 µL, 0.032 mg/µL, 2.5 µmol) was then added and the solution was incubated in a Thermomixer at 37°C for 2 h (800 rpm). The reaction mixture was analyzed by analytical RP-HPLC and isolated by semi-preparative RP-HPLC using Gradient A (Supporting Information). The product, TCO-Z$_{HER3:8698}$, was lyophilized and quantified by measuring the UV absorbance at 280 nm on a Nanodrop 2000 (256.6 µg, 49.8% yield). Analytical RP-HPLC: R$_t$ = 14:11 (min:sec). MALDI-MS (*m/z*) : [M + H]$^+$ expected: 7534, found: 7534.0.

Synthesis of 4-(6-methyl-1,2,4,5-tetrazin-3-yl)benzyl 4-methylbenzenesulfonate (2). A solution of *p*-toluenesulfonyl chloride (122 mg, 0.64 mmol) in DCM (10 mL) was added to compound **1** (87 mg, 0.43 mmol) followed by triethylamine (0.1 mL, 0.80 mmol). The reaction mixture was stirred at ambient temperature for 16 h. The solvent was removed *in vacuo* and the pink solid was purified by flash column chromatography on silica gel (40 - 63 µm, 60 Å). EtOAc/hexane, 2:8) yielding compound **2** as pink powder (66 mg, 43% yield). ^{1}H-NMR (500 MHz, $CDCl_3$): δ = 8.55 (d, *J* = 8.5 Hz, 2H), 7.85 (d, *J* = 8.5 Hz, 2H), 7.49 (d, *J* = 8.3 Hz, 2H), 7.36 (d, *J* = 8.3 Hz, 2H), 5.16 (s, 2H), 3.11 (s, 3H), 2.45 (s, 3H). ^{13}C-NMR (126 MHz, $CDCl_3$): δ = 167.46, 163.64, 145.09, 137.92, 133.03, 132.30, 129.94, 128.88, 128.15, 128.01, 70.85, 21.67, 21.19. ESI-MS *(m/z)*: [M + H]$^+$ calcd for $C_{17}H_{17}N_4O_3S$: 357.4, found: 357.10.

Synthesis of 2,2'-(7-(4-(6-methyl-1,2,4,5-tetrazin-3-yl)benzyl)-1,4,7-triazonane-1,4-diyl)diacetic acid (3). NO2AtBu (99 mg, 0.28 mmol) was added to a solution of compound **2** (66 mg, 0.19 mmol) in acetonitrile (2 mL) followed by DIPEA (0.1 mL, 0.55 mmol) at 0 °C. The reaction was stirred for 24 h at room temperature. The solvent was removed *in vacuo* and TFA (2 mL) was added to the residue. The mixture was stirred at ambient temperature for 3 h. The product was obtained by removing the TFA *in vacuo* as a red oily residue (47 mg, 56% yield). For radiochemistry purposes, the product was further purified by semi-preparative RP-HPLC using Gradient C (Supporting Information). The isolated product was lyophilized to yield a red oil (15 mg, 18% yield). ^{1}H NMR (500 MHz, MeOD-d_4) δ 8.63 (d, *J* = 8.5 Hz, 2H), 7.86 (d, *J* = 8.5 Hz, 2H), 4.45 (s, 2H), 3.58 (d, *J* = 20.4 Hz, 4H), 3.26–3.11 (m, 6H), 3.07 (s, 3H), 3.02–2.91 (m, 4H), 2.87 (s, 2H). ^{13}C NMR (126 MHz, MeOD-d_4) δ 172.48, 167.62, 163.53, 137.51, 133.05, 130.96, 127.96, 116.71, 99.99, 58.67, 54.64, 50.41, 49.51,

19.70. Analytical RP-HPLC (Gradient B): R_t = 9:03 (min:sec). ESI-HRMS: $[M + H]^+$ (m/z) calcd for $C_{20}H_{28}N_7O_4$: 430.2203, found 430.2178.

Radiosynthesis of [^{18}F]AlF-3 and IEDDA reaction with TCO-$Z_{HER3:8698}$. A mixture containing **3** in water (4 µL, 28 nmol), 2 mM $AlCl_3$ in 0.5 M sodium acetate pH 4 (14 µL, 18-28 nmol), non-purified ^{18}F-fluoride (460-500 MBq) and an equal volume of EtOH (or acetonitrile, or *tert*-butanol) was incubated at 100 °C for 15 min. Analytical RP-HPLC (Gradient D, Supporting Information): R_t [^{18}F]AlF-**3** = 7.1 and 7.5 min. Specific activity = 10.6-16.6 GBq/µmol (decay corrected to the end of reaction).
The reaction solution containing [^{18}F]AlF-**3** was quickly added to lyophilized TCO-$Z_{HER3:8698}$ (3.5 nmol, **3** to TCO-$Z_{HER3:8698}$ molar ratio 7:1) and the mixture was incubated at ambient temperature with mixing (800 rpm) for 17 min before purification by RP-HPLC using Gradient A (Supporting Information). The collected fraction containing the product was diluted with 0.1% aq TFA (3 mL) and loaded on an Oasis HLB-SPE cartridge. The trapped radioactivity was washed with 0.1% aq TFA (3 mL) and then eluted with 50% ethanol/water (v/v, 100 µl). The product was quantified by measuring the UV absorbance at 280 nm on a Nanodrop 2000. Synthesis time (from the beginning of the reaction) = *ca* 70 min. The RCC (non-decay corrected) was expressed as the mean of n = 12 experiments ± SD. Protein recovery = 34.0-54.8%

***In vitro* serum stability assay**.[34] The stability of [^{18}F]AlF-NOTA-$Z_{HER3:8698}$ and [^{18}F]AlF-NODA-$Z_{HER3:8698}$, with respect to change in RCP and loss of radioactivity from the affibody molecule, was assessed by incubating the purified [^{18}F]AlF-radioconjugates (*ca* 4 MBq) in mouse serum (500 µL) in a Thermomixer at 37°C for 1 h (300 rpm). The mixture was then precipitated by addition of EtOH (300 µL) and centrifuged at 16000 × g for 2 min at 21°C. DMF (300 µL) was added to the supernatant which was then centrifuged at 16000 × g for 2 min at 21°C. The supernatant was acidified with 0.1% aq TFA (300 µL), filtered through a 0.2 µm Iso-Disc PVDF syringe filter and analyzed by RP-HPLC using Gradient A (Supporting Information). The radioactivity associated with the protein from the centrifuge spins was measured in a dose calibrator. Aqueous non-purified [^{18}F]Fluoride solution (*ca* 4 MBq) incubated in mouse serum (500 µL) was processed in the same way and used as control (to confirm the R_t of free [^{18}F]Fluoride). The experiments were performed in triplicate. The data are expressed as the average of n = 3 measurements ± SEM.

***In vitro* binding affinity and specificity of uptake of the radioconjugates.** The dissociation constants (K_d) of the ^{18}F-radiolabeled conjugates were assessed by a saturation binding assay using the high HER3-expressing MCF-7 cell line. The cells (5×10^5) were plated on 12-well plates and cultured overnight. After removing the growth medium, the cells were washed with PBS and incubated with increasing concentrations of the radioconjugates (final concentrations of 0.01, 0.1, 0.5, 1.0, 2.5, 3.5, and 5.0 nM, *ca* 0.05-37 kBq/well) diluted in non-supplemented DMEM (1 mL). Non-specific binding was determined by pre-incubating the cells with 100-fold molar excess of the non-radiolabeled affibody molecule for 10 min. After 1 h incubation at 4°C, the cells were rinsed twice with PBS prior to detachment with trypsin-EDTA. Afterwards, the cells from each well were transferred to scintillation vials and

the total cell-associated radioactivity measured in a gamma counter. To estimate the K_d, the specific binding was determined by subtracting the fraction of non-specific binding from the total binding. The data were plotted as the amount (nM) of bound *vs* free radioconjugate. The binding curve was fitted to a one-site receptor-binding model using GraphPad Prism 6.00.
The specificity of binding of each radioconjugate was evaluated using MCF-7 and MDA-MB-231 cells (5×10^5) plated on 12-well plates 24 h prior to the experiment. The cells were pre-incubated with a 100-fold molar excess of non-radiolabeled affibody molecule for 10 min at 4°C, followed by incubation with the radioconjugate (1 nM, *ca* 5 kBq/well) for 1 h at 4°C. The cells were rinsed twice with PBS, trypsinized, and collected into scintillation vials. The radioactivity was assessed using a gamma counter. The specificity of binding was normalized to the maximum cell-associated radioactivity per experiment and presented as mean of n = 3 independent measurements ± SEM.

***In vivo* evaluation.** All experiments were performed in compliance with licenses issued under the UK Animals (Scientific Procedures) Act 1986 and following local ethical review. Studies were compliant with the United Kingdom National Cancer Research Institute Guidelines for Animal Welfare in Cancer Research.[49] Female NCr athymic mice (6-8 week-old) were subcutaneously injected on the shoulder with MCF-7 or MDA-MB-231 cells (7.5×10^6/mouse) suspended in 30% Matrigel. For MCF-7 cells, 17β-estradiol pellets (0.72 mg, 90 days release) were implanted 48 h before cell inoculation, and remained in place until the end of the study. Tumors were allowed to grow for 3-4 weeks until reaching 100 mm^3. PET/CT imaging studies were conducted using an Albira PET/SPECT/CT imaging system. Mice were administered the radioconjugate (1 μg in 100 μL of 0.9% sterile saline, 0.7-0.8 MBq/mouse) by intravenous tail vein injection and approximately 5 minutes prior to imaging were anesthetized using isoflurane/O_2 mixture (1.5-2.0 % v/v) and placed prone in the center of the scanner's field of view. Whole body PET static images were acquired 1 h post radioconjugate injection for the duration of 10 min with a 358 to 664 keV energy window, followed by CT acquisition. The image data were normalized to correct for PET non-uniformity, dead-time count losses, positron branching ratio, and physical decay to the time of injection. No attenuation or partial-volume averaging corrections were applied. The PET images were reconstructed using a MLEM algorithm (12 iterations) with a voxel size of $0.5 \times 0.5 \times 0.5$ mm^3. Whole body standard high resolution CT scans were performed with the X-ray tube set-up at a voltage of 45 kV, current of 400 μA and 250 projections (1s per projection) and a voxel size of $0.5 \times 0.5 \times 0.5$ mm^3. The CT images were reconstructed using a FBP algorithm. Image analysis was performed using the PMOD software package.
Immediately after the image data acquisition, the mice were euthanized by cervical dislocation for the biodistribution studies. The major organs/tissues were dissected, weighed, and the radioactivity was measured in a gamma counter. The percentage of the injected dose per gram of tissue (%ID/g) was determined for each organ/tissue. The data are expressed as the average of n = 3 mice ± SD.

ASSOCIATED CONTENT

Supporting Information

The following supporting information is available: Materials and methods, analytical data for tetrazine ($^{1}H/^{13}C$ NMR and ESI-HRMS) and affibody conjugates (MALDI-MS), RP-HPLC conditions and analytical RP-HPLC chromatograms, specific activities table, $logD_{7.4}$ determination, *in vitro* assays (serum stability and binding affinity), and general information about cell culture and the *in vivo* experiments. The material is available free of charge on the ACS Publication website http://pubs.acs.org

ACKNOWLEDGEMENTS

The authors gratefully thank Affibody AB for supplying the affibody molecule. This work was supported by the Cancer Research UK-Cancer Imaging Centre (C1060/A16464) and EPSRC (EP/H046526/1). The authors would like to thank David Turton and Tom Burley for their assistance with experiments and Prof. Keith Jones for his helpful comments. The EPSRC UK National Mass Spectrometry Facility at Swansea University is thanked for provision of technical services.

ABBREVIATIONS

NOTA, 1,4,7-triazacyclononane-1,4,7-triacetate; NODA, 1,4,7-triazacyclononane-1,4-diacetate; TCO, *trans*-cyclooctene; IEDDA; inverse-Electron Demand Diels-Alder; K_d, dissociation constant; RCC, radiochemical conversion; DTT, dithiothreitol; TCEP-HCl, *tris*(2-carboxyethyl)-phosphine hydrochloride; MWCO, molecular weight cut off; NO2AtBu, 2,2'-(1,4,7-Triazacyclononane-1,4-diyl)diacetate; DIPEA, *N*,*N*-diisopropylethylamine; TFA, trifluoroacetic acid; RCP, radiochemical purity; SPE, solid phase extraction; SDS-PAGE, sodium dodecyl sulfate-polyacrylamide gel electrophoresis; EDTA, ethylenediaminetetraacetic acid; p.i.. post injection; MMA-NOTA, maleimido-mono-amide NOTA; R_t, retention time; TCO-PEG_3-Maleimide, *trans*-cyclooctene-(polyethylene glycol)$_3$-maleimide; NaOAc, sodium acetate; DMSO, dimethyl sulfoxide; DCM, dichloromethane; EtOAc, ethyl acetate; EtOH, ethanol; DMF; dimethylformamide; DMEM, Dulbecco's modified eagle medium; HRG, heregulin; SEM, standard error of mean; MLEM, maximum likelihood expectation maximization; FBP, filtered backprojection; SD, standard deviation; RCY, radiochemical yield.

REFERENCES

(1) Jiang, N., Saba, N. F., and Chen, Z. G. (2012) Advances in targeting HER3 as an anticancer therapy. *Chemother. Res. Pract.*, DOI:10.1155/2012/817304.

(2) Marmor, M. D., Skaria, K. B., and Yarden, Y. (2004) Signal transduction and oncogenesis by ErbB/HER receptors. *Int. J. Radiat. Oncol. Biol. Phys. 58*, 903-913.

(3) Hsieh, A. C., and Moasser, M. M. (2007) Targeting HER proteins in cancer therapy and the role of the non-target HER3. *Br. J. Cancer 97*, 453-457.

(4) Mujoo, K., Choi, B.-K., Huang, Z., Zhang, N., and An, Z. (2014) Regulation of ERBB3/HER3 signaling in cancer. *Oncotarget 5*, 10222-10236.

(5) Holbro, T., Beerli, R. R., Maurer, F., Koziczak, M., Barbas, C. F., and Hynes, N. E. (2003) The ErbB2/ErbB3 heterodimer functions as an oncogenic unit: ErbB2 requires ErbB3 to drive breast tumor cell proliferation. *Proc. Natl. Acad. Sci. U.S.A. 100*, 8933-8938.

(6) Baselga, J., and Swain, S. M. (2009) Novel anticancer targets: revisiting ERBB2 and discovering ERBB3. *Nat. Rev. Cancer 9*, 463-475.

(7) Campbell, M. R., Amin, D., and Moasser, M. M. (2010) HER3 comes of age: new insights into its functions and role in signaling, tumor biology, and cancer therapy. *Clin. Cancer Res. 16*, 1373-1383.

(8) Lee-Hoeflich, S. T., Crocker, L., Yao, E., Pham, T., Munroe, X., Hoeflich, K. P., Sliwkowski, M. X., and Stern, H. M. (2008) A central role for HER3 in *HER2*-amplified breast cancer: implications for targeted therapy. *Cancer Res. 68*, 5878-5887.

(9) Navolanic, P. M., Steelman, L. S., and McCubrey, J. A. (2003) EGFR family signaling and its association with breast cancer development and resistance to chemotherapy. *Int. J. Oncol. 22*, 237-252.

(10) Sergina, N. V., Rausch, M., Wang, D., Blair, J., Hann, B., Shokat, K. M., and Moasser, M. M. (2007) Escape from HER-family tyrosine kinase inhibitor therapy by the kinase-inactive HER3. *Nature 445*, 437-441.

(11) Kruser, T. J., and Wheeler, D. L. (2010) Mechanisms of resistance to HER family targeting antibodies. *Exp. Cell Res. 316*, 1083-1100.

(12) Schoeberl, B., Faber, A. C., Li, D., Liang, M.-C., Crosby, K., Onsum, M., Burenkova, O., Pace, E., Walton, Z., Nie, L.*, et al.* (2010) An ErbB3 antibody, MM-121, is active in cancers with ligand-dependent activation. *Cancer Res. 70*, 2485-2494.

(13) Schaefer, G., Haber, L., Crocker, L. M., Shia, S., Shao, L., Dowbenko, D., Totpal, K., Wong, A., Lee, C. V., Stawicki, S.*, et al.* (2011) A two-in-one antibody against HER3 and EGFR has superior inhibitory activity compared with monospecific antibodies. *Cancer Cell 73*, 5183-5194.

(14) LoRusso, P., Jänne, P. A., Oliveira, M., Rizvi, N., Malburg, L., Keedy, V., Yee, L., Copigneaux, C., Hettmann, T., Wu, C.*, et al.* (2013) Phase I study of U3-1287, a fully human anti-HER3 monoclonal antibody, in patients with advanced solid tumors. *Clin. Cancer Res. 19*, 3078-3087.

(15) Meulendijks, D., Jacob, W., Martinez-Garcia, M., Taus, A., Lolkema, M. P., Voest, E. E., Langenberg, M. H. G., Kanonnikoff, T. F., Cervantes, A., De Jonge, M. J.*, et al.* (2016) First-in-human Phase I study of Lumretuzumab, a glycoengineered humanized anti-HER3 monoclonal antibody, in patients with metastatic or advanced HER3-positive solid tumors. *Clin. Cancer Res. 22*, 877-885.

(16) Terwisscha van Scheltinga, A. G. T., Lub-de Hooge, M. N., Abiraj, K., Schröder, C. P., Pot, L., Bossenmaier, B., Thomas, M., Hölzlwimmer, G., Friess, T., Kosterink, J. G. W.*, et al.* (2014) ImmunoPET and biodistribution with human epidermal growth factor receptor 3 targeting antibody ^{89}Zr-RG7116. *mAbs 6*, 1051-1058.

(17) Lockhart, A. C., Liu, Y., Dehdashti, F., Laforest, R., Picus, J., Frye, J., Trull, L., Belanger, S., Desai, M., Mahmood, S.*, et al.* (2015) Phase 1 evaluation of [^{64}Cu]DOTA-Patritumab to assess dosimetry, apparent receptor occupancy, and safety in subjects with advanced solid tumors. *Mol. Imaging Biol. 17*, 1-8.

(18) Wehrenberg-Klee, E., Turker, N. S., Heidari, P., Larimer, B., Juric, D., Baselga, J., Scaltriti, M., and Mahmood, U. (2016) Differential receptor tyrosine kinase PET imaging for therapeutic guidance *J. Nucl. Med.*, DOI:10.2967/jnumed.2115.169417.

(19) Göstring, L., Malm, M., Höidén-Guthenberg, I., Frejd, F. Y., Ståhl, S., Löfblom, J., and Gedda, L. (2012) Cellular effects of HER3-specific affibody molecules. *PLoS One*, DOI:10.1371/journal.pone.0040023.

(20) Orlova, A., Feldwisch, J., Abrahmsén, L., and Tolmachev, V. (2007) Affibody molecules for molecular imaging and therapy for cancer. *Cancer Biother. Radiopharm. 22*, 573-584.

(21) Malm, M., Kronqvist, N., Lindberg, H., Gudmundsdotter, L., Bass, T., Frejd, F. Y., Höidén-Guthenberg, I., Varasteh, Z., Orlova, A., Tolmachev, V*., et al.* (2013) Inhibiting HER3-mediated tumor cell growth with affibody molecules engineered to low picomolar affinity by position-directed error-prone PCR-like diversification. *PLoS One*, DOI: 10.1371/journal.pone.0062791.

(22) Orlova, A., Malm, M., Rosestedt, M., Varasteh, Z., Andersson, K. G., Kumar Selvaraju, R., Altai, M., Honarvar, H., Strand J., Ståhl, S*., et al.* (2014) Imaging of HER3-expressing xenografts in mice using a $^{99m}Tc(CO)_3$-HEHEHE-$Z_{HER3:08699}$ affibody molecule. *Eur. J. Nucl. Med. Mol. Imaging 41*, 1450-1459.

(23) Andersson, K. G., Rosestedt, M., Varasteh, Z., Malm, M., Sandström, M., Tolmachev, V., Löfblom, J., Ståhl, S., and Orlova, A. (2015) Comparative evaluation of 111In-labeled NOTA-conjugated affibody molecules for visualization of HER3 expression in malignant tumors. *Oncol. Rep. 34*, 1042-1048.

(24) Robinson, M. K., Hodge, K. M., Horak, E., Sundberg, Å. L., Russeva, M., Shaller, C. C., von Mehren, M., Shchaveleva, I., Simmons, H. H., Marks, J. D*., et al.* (2008) Targeting ErbB2 and ErbB3 with a bispecific single-chain Fv enhances targeting selectivity and induces a therapeutic effect *in vitro*. *Br. J. Cancer 99*, 1415-1425.

(25) Tolmachev, V., Wållberg, H., Sandström, M., Hansson, M., Wennborg, A., and Orlova, A. (2011) Optimal specific radioactivity of anti-HER2 Affibody molecules enables discrimination between xenografts with high and low HER2 expression levels. *Eur. J. Nucl. Med. Mol. Imaging 38*, 531-539.

(26) Zeng, J.-L., Wang, J., and Ma, J.-A. (2015) New strategies for rapid ^{18}F-radiolabeling of biomolecules for radionuclide-based in vivo imaging. *Bioconj. Chem. 26*, 1000-1003.

(27) McBride, W. J., Sharkey, R. M., Karacay, H., D'Souza, C. A., Rossi, E. A., Laverman, P., Chang, C.-H., Boerman, O. C., and Goldenberg, D. M. (2009) A novel method of ^{18}F radiolabeling for PET. *J. Nucl. Med. 50*, 991-998.

(28) Jacobson, O., Kiesewetter, D. O., and Chen, X. (2015) Fluorine-18 radiochemistry, labeling strategies and synthetic routes. *Bioconj. Chem. 26*, 1-18.

(29) Liu, S., Liu, H., Jiang, H., Xu, Y., Zhang, H., and Cheng, Z. (2011) One-step radiosynthesis of ^{18}F-AlF-NOTA-RGD_2 for tumor angiogenesis PET imaging. *Eur. J. Nucl. Med. Mol. Imaging 38*, 1732-1741.

(30) McBride, W. J., Sharkey, R. M., and Goldenberg, D. M. (2013) Radiofluorination using aluminium-fluoride ($Al^{18}F$). *Eur. J. Nucl. Med. Mol. Imaging*, DOI: 10.1186/2191-219X-3-36.

(31) Niu, G., Lang, L., Kiesewetter, D. O., Ma, Y., Sun, Z., Guo, N., Guo, J., Wu, C., and Chen, X. (2014) In vivo labeling of serum albumin for PET. *J. Nucl. Med. 55*, 1-7.

(32) Heskamp, S., Laverman, P., Rosik, D., Boschetti, F., van der Graaf, W. T. A., Oyen, W. J. G., van Laarhoven, H. w. M., Tolmachev, V., and Boerman, O. C. (2012) Imaging of human epidermal growth factor receptor type 2 expression with ^{18}F-labeled affibody molecule $Z_{HER2:2395}$ in a mouse model for ovarian cancer. *J. Nucl. Med. 53*, 146-153.

(33) Glaser, M., Iveson, P., Hoppmann, S., Indrevoll, B., Wilson, A., Arukwe, J., Danikas, A., Bhalla, R., and Hiscock, D. (2013) Three methods for ^{18}F labeling of the HER2-binding affibody molecule $Z_{HER2:2891}$ including preclinical assessment. *J. Nucl. Med. 54*, 1981-1988.

(34) Su, X., Cheng, K., Jeon, J., Shen, B., Venturin, G. T., Hu, X., Rao, J., Chin, F. T., Wu, H., and Cheng, Z. (2014) Comparison of two site-specifically ^{18}F-labeled affibodies for PET imaging of EGFR positive tumors. *Mol. Pharmaceutics 11*, 3947-3956.

(35) Meyer, J.-P., Houghton, J. L., Kozlowski, P., Abdel-Atti, D., Reiner, T., Pillarsetty, N., Scholz, W., Zeglis, B. M., and Lewis, L. S. (2016) ^{18}F-Based pretargeted PET imaging based on biorthogonal Diels-Alder click chemistry. *Bioconj. Chem. 27*, 298-301.

(36) D'Souza, C. A., McBride, W. J., Sharkey, R. M., Todaro, L. J., and Goldenberg, D. M. (2011) High-yielding aqueous ^{18}F-labeling of peptides via $Al^{18}F$ chelation. *Bioconj. Chem. 22*, 1793-1803.

(37) McBride, W. J., D'Souza, C. A., Sharkey, R. M., and Goldenberg, D. M. (2012) The radiolabeling of proteins by the [^{18}F]AlF method. *Appl. Radiat. Isotopes 70*, 200-2004.

(38) Kiesewetter, D. O., Kramer-Marek, G., Ma, Y., and Capala, J. (2008) Radiolabeling of HER2 specific Affibody® molecule with F-18. *J. Fluor. Chem. 129*, 799-805.

(39) Knall, A.-C., and Slugovc, C. (2013) Inverse electron demand Diels-Alder (iEDDA)-initiated conjugated: a (high) potential click chemistry scheme. *Chem. Soc. Rev. 42*, 5131-5142.

(40) Jewett, J. C., and Bertozzi, C. R. (2010) Cu-free click cycloaddition reactions in chemical biology. *Chem. Soc. Rev. 39*, 1272-1279.

(41) Shetty, D., Choi, S. Y., Jeong, J. M., Lee, J. Y., Hoigebazar, L., Lee, Y.-S., Lee, D. S., Chung, J.-K., Lee, M. C., and Chung, Y. K. (2011) Stable aluminium fluoride chelates with triazacyclononane derivatives proved by X-ray crystallography and ^{18}F-labeling study. *Chem. Commun. 47*, 9732-9734.

(42) Gong, H., Kovar, J., Little, G., Chen, H., and Olive, D. M. (2010) *In vivo* imaging of xenograft tumors using an epidermal growth factor receptor-specific affibody molecule labeled with a near-infrared fluorophore. *Neoplasia 12*, 139-149.

(43) Yang, J., Karver, M. R., Li, W., Sahu, S., and Devaraj, N. K. (2012) Metal-catalyzed one-pot synthesis of tetrazines directly from aliphatic nitriles and hydrazine. *Angew. Chem. Int. Ed. 51*, 5222–5225.

(44) Selvaraj, R., and Fox, J. M. (2013) *trans*-Cyclooctene-a stable, voracious dienophile for bioorthogonal labeling. *Curr. Opin. Chem. Biol. 17*, 753-760.

(45) Löfblom, J., Feldwisch, J., Tolmachev, V., Carlsson, J., Ståhl, S., and Frejd, F. Y. (2010) Affibody molecules: Engineered proteins for therapeutic, diagnostic and biotechnological applications. *FEBS Lett. 584*, 2670-2680.

(46) Singh, J. K., Solanki, A., Maniyar, R. C., Banerjee, D., and Shirsath, V. S. (2012) Rapid equilibrium dialysis (RED): an *in-vitro* high-troughput screening technique for plasma protein binding using human and rat plasma. *J. Bioequiv. Availab. S14*, DOI: 10.4172/jbb.S4114-4005.

(47) Behr, T. M., Goldenberg, D. M., and Becker, W. (1998) Reducing the renal uptake of radiolabeled antibody fragments and peptides for diagnosis and therapy: present status, future prospects and limitations. *Eur. J. Nucl. Med. 25*, 201-212.

(48) Rosestedt, M., Andersson, K. G., Mitran, B., Tolmachev, V., Löfblom, J., Orlova, A., and Ståhl, S. (2015) Affibody-mediated PET imaging of HER3 expression in malignant tumours. *Sci. Rep. 5*, DOI: 10.1038/srep15226.

(49) Workman, P., Aboagye, E. O., Balkwill, F., Balmain, A., Bruder, G., Chaplin, D. J., Double, J. A., Everitt, J., Farningham, D. A. H., Glennie, M. J*., et al.* (2010) Guidelines for the welfare and use of animals in cancer research. *Br. J. Cancer 102*, 1555–1577.